analytical chemistry

Article

pubs.acs.org/ac

Nanopore-Based Electrical and Label-Free Sensing of Enzyme Activity in Blood Serum

Mikiembo Kukwikila[†,‡] and Stefan Howorka*[,†]

[†]Department of Chemistry, Institute of Structural and Molecular Biology, University College London, London, England, United Kingdom

[‡]School of Chemistry, University of Southampton, Southampton, England, United Kingdom

Supporting Information

ABSTRACT: A generic strategy to expand the analytical scope of electrical nanopore sensing is presented. We specifically and electrically detect the activity of a diagnostically relevant hydrolytic enzyme and remove the analytically harmful interference from the biochemically complex sample matrix of blood serum. Our strategy is demonstrated at the example of the renin protease which is involved in regulation of blood pressure. The analysis scheme exploits a new approach to reduce sample complexity while generating a specific read-out signal. Within a single spin-column (i), the protease cleaves a resin-tethered peptide substrate (ii) which is affinity-purified using the same multifunctional resin to remove interfering blood serum components, followed by (iii) detecting the peptide via electrical nanopore recordings. Our approach is beneficial in several ways. First, by eliminating serum components, we overcome limitations of nanopore sensing when challenging samples lead to membrane instability and a poor signal-to-noise ratio. Second, the label-free sensing avoids drawbacks of currently used radiolabel-immunoassays for renin. Finally, the strategy of simultaneous generation and purification of a signal peptide within a multifunctional resin can very likely be expanded to other hydrolytic enzymes dissolved in any analyte matrix and exploited for analytical read-out methods other than nanopore sensing.

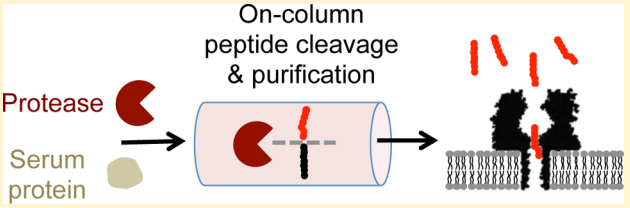

Nanopore analytics is an increasingly popular approach to detect molecules in a label-free fashion. The sensing principle with nanopores is simple yet powerful. Individual molecules pass through or interact with a single pore of nanoscale diameter thereby causing detectable changes in ionic pore current (Figure 1A).[1−3] Detecting individual molecules has advantages over ensemble measurements. For example, subpopulations of analytes can be uncovered as well as the molecules' shape, size, or net charge. The approach is generic and can be implemented with different types of nanopores. These include biological protein pores embedded into a lipid bilayer as well as with man-made solid-state pores drilled into thin membranes composed of SiN, glass, or organic polymers.[1] Reflecting its generic principle, nanopore analytics can be exploited for the specific and label-free sensing of nucleic acid[4−8] including DNA sequencing,[9,10] the detection of proteins,[11−14] and enzymatic activity and peptides,[15−19] which are of relevance to the present report.[5]

Despite the advances, sensing of analytes in biological samples with a complex analyte matrix remains challenging. One issue is the often dramatic increase in the background signal triggered by nonanalyte molecules of the matrix which unspecifically block the nanopore, as schematically illustrated in Figure 1B. This is of particular importance for pores without analyte receptors as these help enhance the strength of the specific signal.[20,21] Another problem is the instability of lipid bilayers which are disrupted by amphiphilic proteins[22,23] found, e.g., in blood-derived samples (Figure 1B). Lipid bilayers can be physically stabilized[23] but remain biochemically labile. Another possible route is to replace biological pores with inert solid-state nanopore membranes.[1,24−26] However, the diameter of these pores is usually too wide for relatively small peptide analytes,[27,28] and peptide detection based on ionic current blockades has, to our knowledge, not been experimentally achieved with solid-state pores. Protein or DNA-origami pores can be inserted into solid-state pores[29,30] to narrow the effective pore diameter, but the higher noise level hinders the sensing of very small analytes such as peptides.

Here, we present a new nanopore-based strategy to specifically sense enzymatic activity present in a matrix containing serum proteins. The approach combines several beneficial features and overcomes the issue of membrane instability while maintaining sensitivity and reducing non-specific background signal. The sensing strategy is exemplified at the biochemical analyte renin. Renin is a protease enzyme which mediates the regulation of blood pressure and homeostasis[31] by generating peptide-based hormones via proteolysis. The natural substrate of renin is the pro-hormone angiotensinogen. Proteolytic cleavage by renin releases the biologically active N-terminal 10 amino acid-long peptide angiotensin I

Received: March 27, 2015
Accepted: June 8, 2015
Published: August 25, 2015

DOI: 10.1021/acs.analchem.5b01764
Anal. Chem. 2015, 87, 9149−9154

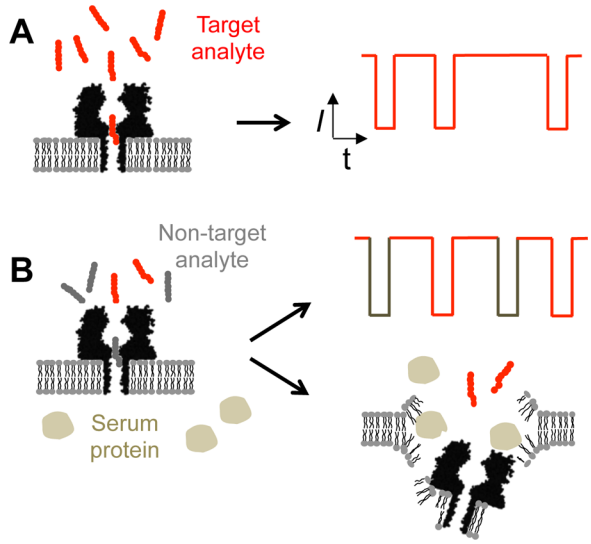

Figure 1. Scheme illustrating the principle and challenges of electrical nanopore sensing. (A) The sensing approach relies on the translocation of target analytes through a lipid bilayer-embedded nanopore giving rise to time-dependent blockades of the ionic pore current, *I*. (B) Undesired background signals are caused by nontarget molecules in the sample (top). Components of the analyte matrix such as serum proteins rupture the bilayer membrane (bottom).

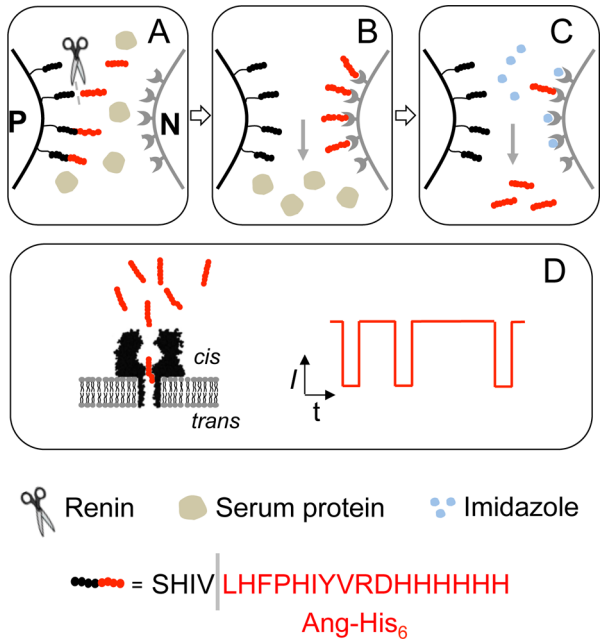

Figure 2. Scheme illustrating the sensing strategy for the protease renin. It involves (A) the enzymatic cleavage of the substrate peptide fragment Ang-His_6 (red) from beads P and simultaneous affinity binding to beads N carrying Ni^{2+}-NTA groups, (B) removal of serum proteins by washing, (C) elution of the Ang-His_6 peptide, and (D) electrical sensing of the peptide using the membrane nanopore α-hemolysin. Steps A–C are conducted using one spin column containing a mixture of beads P and N.

which in turn can be fragmented into smaller hormones. Given its role as signaling gate-keeper, renin activity in serum is a useful clinical indicator of hypertension. Currently used approaches to detect renin are based on radioactivity-based immunoassays to either determine the amount of renin or measure its activity via the proteolytically cleaved peptide substrates.[32−34] By comparison, our new nanopore-based strategy is label-free and less complex. We demonstrate its viability by detecting renin at high specificity and sensitivity. We expect that the advantages of our analytical route are widely applicable to sense several other hydrolytic enzymes in complex sample matrices.

RESULTS AND DISCUSSION

The principle of the sensing strategy for renin features two functional modules: signal generation and signal sensing. Both are schematically illustrated in Figure 2A–C and Figure 2D, respectively. Briefly, signal generation is achieved by adding renin-containing blood serum to microscale beads P displaying a substrate peptide (Figure 2A) derived from angiotensinogen. After renin-mediated cleavage, peptide fragment Ang-His_6 (Figure 2A, indicated in red) binds with its engineered hexahistidine tag specifically to Ni^{2+}-NTA-beads, N, while membrane-destabilizing serum proteins are removed by washing (Figure 2B) so that purified peptide Ang-His_6 can be eluted (Figure 2C). The signal generation module hence features a uniquely designed peptide substrate for surface-tethered peptide cleavage and purification using two types of beads within a single spin column. This is novel and simplifies handling as signal generation can be carried out in a simple fashion. In the subsequent module for signal sensing (Figure 2D), the eluted peptide fragments are detected as they pass a protein nanopore and give rise to transient blockades in the ionic pore current.

The substrate beads P were carefully designed to achieve specific and efficient cleavage by renin. The substrate peptide HO-SHIV/LHFPHIYVRD-$HHHHHH-NH_2$ (Figure 2, cleavage site indicated by a slash) was derived from the N-terminus of angiotensinogen.[35] The underlined substrate sequence (corresponding to amino acid position 14 to 1 of angiotensinogen[35,36]) is long enough to ensure specific recognition by renin without interference by the engineered His_6 tag at the peptide's N terminus.[37−39] To further improve steric accessibility, the peptide was C-terminally linked to beads via a flexible polyethylene glycol-based linker.[40] Steric accessibility to the peptide substrate was also designed to be high as the beads were composed of polyacrylamide which can swell in water to permit the permeation by proteins with a mass of up to 35 kDa which includes renin.[41]

The tethered substrate was specifically recognized and cleaved by renin as shown by HPLC analysis of the released soluble Ang-His_6. For reasons of simplicity, the digestion was conducted first with isolated beads P and renin but in the absence of serum components or beads N. The HPLC traces of the supernatants of the cleavage mixtures (Figure 3A) feature a unique peak at 16 min which increases in magnitude with longer incubation times (Figure 3A, B). The peak represents soluble Ang-His_6 fragment released by renin activity, as confirmed by mass spectrometry (see the Supporting Information). In control experiments, no peptide peak was observed in the absence of renin or when the non-recognizing enzyme trypsin was used (data not shown) confirming the specificity of the renin-mediated cleavage. The second major peak in the kinetic HPLC traces at 20 min (Figure 3B) represents protein BSA which is included to stabilize renin. We note that incubation durations of several hours to overnight are common for the existing renin assays.[32−34]

DOI: 10.1021/acs.analchem.5b01764
Anal. Chem. 2015, 87, 9149−9154

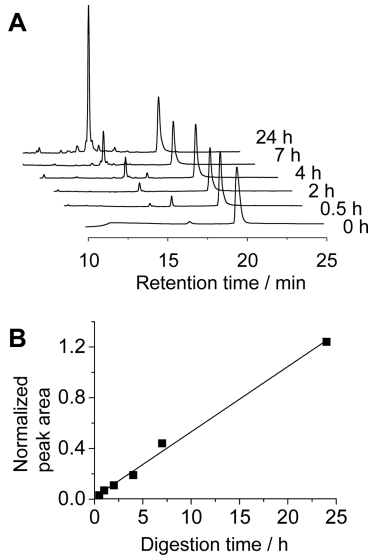

Figure 3. Renin cleaves peptide fragment Ang-His$_6$ from beads P as shown by HPLC analysis. (A) HPLC traces of digestion solutions incubated for the indicated durations. Beads P were removed prior to analysis of the sample. (B) The area of the Ang-His$_6$ peak at 16 min retention time increases with the duration of the enzymatic digestion. The peak area was normalized to the BSA peak with a retention time of 20 min. The data represent the averages of two independent experiments.

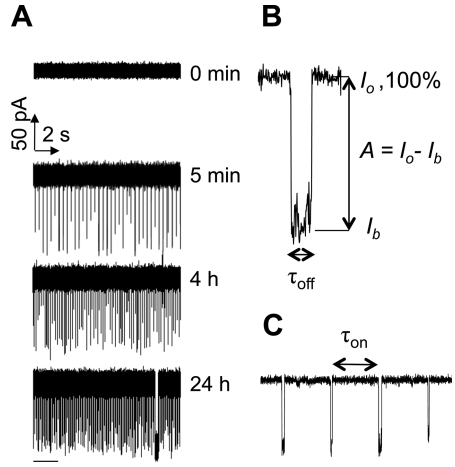

Figure 4. Peptide Ang-His$_6$ causes clear current blockades in nanopore recordings. (A) Single-channel current traces of the αHL pore without peptide (0 min) and with peptide solution from the renin-digestion of Figure 3 for the indicated durations. The latter traces were acquired in the variable-length mode of nanopore acquisition software pClamp and subjected to data reduction. In variable-length mode, segments of the trace without blockade events are removed to yield a concatenated series of blockades. Events with an amplitude of 25% or higher were included. The three traces display events recorded within 100 s which is different from the duration of the concatenated event segments. (B) An individual current blockade event with duration τoff and amplitude A defined by the difference between the open-channel current, I_o, and the current level for the blocked channel, I_b. (C) The interevent interval, τ_{on}, between separate currents is used to calculate their frequency of occurrence, f, using $f = 1/\tau_{on}$.

The enzymatically derived Ang-His$_6$ solutions were analyzed with nanopore recordings (i) to establish that the peptide solutions give rise to clear current electrical signals. Additional objectives were (ii) to confirm the signals' molecular origin by comparison to synthetic peptide analogues and (iii) to demonstrate that increasing peptide concentrations from a longer enzyme incubation lead to more frequent signals. The electrical recordings were conducted with the α-hemolysin (αHL) protein pore (Figure 2D) which is of known X-ray structure[42] and widely used in nanopore analytics.[1] A single αHL nanopore was inserted in a lipid bilayer, and electrical nanopore recordings were performed using standard electrolyte conditions (1 M KCl and 50 mM Tris, pH 8.2). Flow of ionic current was induced by applying a potential of +100 mV at the *trans* side of the αHL pore with the *cis* side grounded (Figure 2D). At these conditions, the αHL pore displayed a current of 105.4 ± 6.6 pA (Figure 4A, 0 min) (n = 10; n, number of independent recordings). Addition of the peptide solution to the *cis* side caused short current blockades (Figure 4A; 5 min, 4 h, 24 h). The clear current signals (Figure 4B) most likely represent the translocation of individual peptides from the *cis* to the positively polarized *trans* side of the pore. The signals do not stem from BSA as the protein with dimensions of approximately 6 × 5 × 4 nm cannot enter the 2.9 nm-wide *cis* pore entrance. Indeed, control recordings with a BSA solution did not give rise to blockades found for Ang-His$_6$ (data not shown).

We characterized the blockades' average amplitude, A, and duration, τ_{off}, and compared them to signals obtained for the synthetically derived peptide fragment Ang-His$_6$. The parameters A and τ_{off} are defined in Figure 4B, and the corresponding histograms for the analysis are shown in the Supporting Information, Figure S1. The amplitude of the enzyme-released peptide had a magnitude of 81.6 ± 2.6% (n = 3) of the open channel. This is close to A for the synthetic Ang-His$_6$ (78.6 ± 2.5%, n = 4; Supporting Information, Figure S2) and also within the data range found for other short oligopeptides.[17,18,43−45] Similarly, the distribution of the amplitudes in the single-channel histograms was wide (Supporting Information, Figure S2), as would be expected for conformationally flexible peptides, compared to the narrow distribution of DNA strands.[46−48] The value for τ_{off} with 0.62 ± 0.18 ms was within the margin of error for the synthetic peptide, 1.02 ± 0.32 ms (Supporting Information, Figure S2), and in line with the time scales for the translocation of other peptides.[17,18,43−45]

The frequencies of occurrence of the electrical signals for the enzymatically released Ang-His$_6$ (Figure 4A) were determined and compared to the kinetic HPLC data. The frequencies are obtained from the inverse of the characteristic inter-event interval, τ_{on} (Figure 4C). In line with expectations, more frequent current blockades were observed for higher peptide concentrations from longer renin incubation times resulting in a good correlation between both data sets (Supporting Information, Figure S1A, Table S1). For example, the frequency of occurrence increased from 0.02 ± 0.009 s^{-1} at a 5 min incubation approximately 20-fold to 0.39 ± 0.04 s^{-1} at 24 h. Importantly, the frequencies of the enzymatically released Ang-His$_6$ were comparable in value to the synthetic peptide once normalized to the corresponding peptide concentrations in the electrolyte solution of the recording chamber. For example, the signal for the sample with a 24 h incubation had a frequency of 0.08 ± 0.02 s^{-1} μM^{-1} which is close to the value of 0.10 ± 0.03 s^{-1} μM^{-1} (n = 3) for the synthetic peptide.

We note that the signal frequency can be increased by tuning experimental parameters such as electrolyte gradient and larger transmembrane voltage. Both factors can enhance the electrophoretic channeling of peptides into the pore. The effect of the

DOI: 10.1021/acs.analchem.5b01764
Anal. Chem. 2015, 87, 9149−9154

gradient across the bilayer is mediated via magnified electric field and was pioneered for DNA strands.[49] When adapted to the synthetic Ang-His_6 peptide, the salt gradient of 0.2 M *cis*/3.8 M KCl *trans* resulted in a 3.9-fold increase of the signal frequency to a value of 0.39 ± 0.07 s^{-1} μM^{-1} (n = 3) compared to symmetric conditions at 1 M KCl. The effect is smaller than previously observed for DNA but in line with the lower charge density (isoelectric point of 7.28) and smaller electrophoretic force for the peptide. The signal frequency was further boosted 2.5-fold by doubling the transmembrane voltage from 100 to 200 mV. Hence, both salt gradient and a higher potential raised the signal frequency approximately 10-fold from 0.10 ± 0.03 to 1.03 ± 0.22 s^{-1} μM^{-1} (n = 3). This increase is of interest when attempting to further increase the sensitivity of the electrical recordings.

After detecting renin activity via cleaved peptides and nanopores read-out, we next probed whether the sensing approach can be applied to renin within human blood serum. We spiked the serum with renin and incubated the mixture with angiotensinogen-His_6 carrying beads and Ni^{2+}-NTA carrying N-beads. As schematically illustrated in Figure 2A–C, this procedure is expected to achieve renin-mediated cleavage of fragment Ang-His_6 as well as the fragment's binding via the His_6-tag to the Ni^{2+}-NTA-beads. Washing is expected to lead to removal of the serum proteins. In contrast, Ang-His_6 can later be released from the N-beads by elution with imidazole which competes for binding in the metal chelate bridge with histidine.

The procedure successfully eliminated the majority of the serum protein content, as shown by sodium dodecyl sulfate-polyacrylamide gel electrophoresis (SDS-PAGE) analysis for the sample before (Figure 5A, lane SAM) and after purification (Figure 5A, EL1). The effective removal was most drastic for albumin with a molecular weight of around 65 kDa (Figure 5A). Quantitative analysis via the Bradford protein assay established that the purification procedure lowered the protein content over 300-fold from 140.3 to 0.47 mg mL^{-1}.

Complementary HPLC analysis of the eluate confirmed that the cleaved substrate fragment Ang-His_6 was successfully eluted (Figure 5B; trace Ang-H_6, el.). As expected for specific cleavage, the HPLC peak eluted at the same position as synthetic Ang-His_6 (Figure 5B; Ang-H_6 syn). Furthermore, renin rather than nonspecific hydrolysis caused fragmentation, as illustrated by a control experiment without enzyme but with serum (Figure 5B, blank). It is also certain that the eluted peptide peak solely represents Ang-His_6 rather than any other peptides such as the substrate angiotensinogen-His_6 as both synthetic peptides have different HPLC retention times (Figure 5B, Ang-His_6 and A-His_6). MALDI MS analysis confirmed the expected chemical identity of the Ang-His_6 peak (Supporting Information, Figure S5). HPLC analysis of the peak areas furthermore quantified the amount of Ang-His_6 peptide purified with N-beads using a calibration curve setup using the synthetic peptide of known concentration to provide a reference standard for comparison to nanopores recordings.

The presence of the Ang-His_6 peptide in the solution was confirmed by nanopore recordings. The current blockades obtained when adding the eluate to the *cis* side of the αHL pore (Figure 6A) had an average blockade amplitude of 76 ± 4% and duration of 0.68 ± 0.22 ms (n = 4) (Supporting Information, Figure S3) consistent with the characteristics of events previously obtained for synthetic as well as enzymatically released but unpurified peptide. Furthermore, the frequency of occurrence for the purified peptides was 0.12 ± 0.03 s^{-1} μM^{-1} after normalization to the peptide concentration obtained from HPLC analysis. This frequency of occurrence is in good agreement with the value obtained for recordings with the reference standard of the synthetic peptide 0.10 ± 0.03 s^{-1} μM^{-1}. Nanopore recordings finally established that the presence of serum protein in unpurified samples lead to rupturing of the lipid bilayer membranes (Supporting Information, Figure S4), thereby underscoring the necessity to remove the destabilizing proteins in order to conduct successful nanopores measurements.

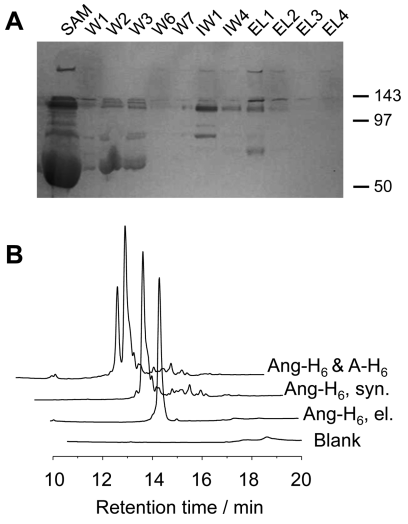

Figure 5. Renin-mediated liberation of Ang-His_6 and purification from serum proteins using one column containing beads P and N. (A) SDS polyacrylamide electropherogram illustrating the removal of serum proteins. The lanes show the initial sample (SAM), fractions after column washes with water (W1–3 and W6–7) and 10 mM imidazole-containing buffer (IW1 and IW4), and eluates using 250 mM imidazole solution (EL1–4). The position of the molecular weight markers in kDa is indicated at the right side of the gel image. (B) HPLC traces of the EL1 eluate stemming from the digestion/purification protocol (Ang-H_6, el.), a control without renin (Blank), a synthetic version of the peptide cleavage product (Ang-H_6, syn.), and a mixture of synthetic peptide Ang-His_6 and substrate angiotensinogen (Ang-H_6 and A-H_6).

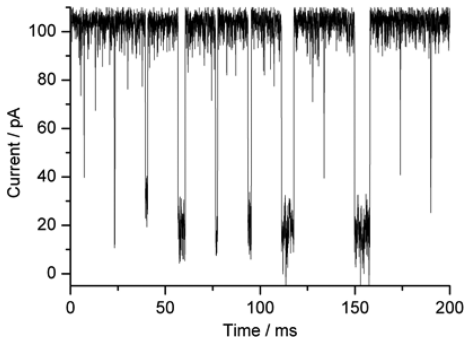

Figure 6. Ang-His_6 peptide that has been cleaved by renin and purified from serum proteins leads to blockade events of the αHL pore. The analyzed sample is the EL1 eluate from Figure 5. The nanopore recording was obtained in the variable-length mode where segments of the trace without blockade events are removed to yield a concatenated series of blockades. The threshold for including events was a blockade amplitude of 25% or higher.

DOI: 10.1021/acs.analchem.5b01764
Anal. Chem. 2015, 87, 9149–9154

Here, we have presented a new approach to detect hydrolytic enzyme activity. The enabling core of the strategy is the use of a rationally designed substrate in combination with solid-phase digestion and purification. The advantages of the approach include the simplification of sample processing, the facile generation of a specific target signal, the simultaneous reduction of background noise, and the removal of other undesired contaminants which otherwise interfere with the signal detection. The strategy was demonstrated for enzyme renin but should in principle be applicable to all other hydrolytic enzymes, including peptidases, protease, nucleases, glyosylases, and other biopolymer-cleaving enzymes as well as esterases, amidases, and enzymes that cleave bonds, provided the chemical substrate is designed to facilitate solid-phase digestion and purification. Our strategy was exemplified with nanopore analysis but could be expanded to other read-out techniques that benefit from the simplification of the sample complexity.

EXPERIMENTAL SECTION

Synthesis of Soluble and Resin-Linked Peptides. The soluble peptides angiotensinogen-His_6 and angiotensin-His_6 and PEGA resin-linked angiotensinogen-His_6 were synthesized using Fmoc solid-phase peptide synthesis as described in the Supporting Information.

HPLC Analysis. HPLC analysis was performed using a reverse phase Varian ProStar system with a Model 210 solvent delivery mode and a Model 320 dual wavelength detector. The mobile phase A consisted of 0.1% (v/v) TFA in water and mobile phase B was 0.1% (TFA) in acteonitrile. The UV absorbance was monitored at 214 and 254 nm. Analytical analysis was performed using a Varian Pursuit XRS C18 column (250 × 4.6 mm). The gradient started with 2% eluent B and rose linearly to 60% B over 20 min with a flow rate of 1 mL min^{-1}. Semipreparative purification was performed using a Phenomenex Luna C18 column (250 × 10 mm). The gradient started with 2% eluent B and rose linearly to 60% B over 30 min with a flow rate of 5 mL min^{-1}. Fractions containing the correct peak were pooled; the solvent was removed under reduced pressure to approximately 1 mL, and the solution was lyophilized overnight. The purity of the peptides was assessed using analytical HPLC and MS analysis.

MS Analysis. ESI-MS analysis was performed using a Waters Aquity Ultra performance LC-MS system equipped with an Aquity UPLC BEH C18 column (50 × 2.1 mm, 1.7 mm beads). MALDI-MS analysis was performed using a Waters Micro MX machine. For MALDI analysis, the peptides were concentrated and desalted via aspiration through C18 Ziptip tips (Millipore) and eluted using a 50% ACN solution. The eluted peptides were mixed with an α-cyano-4-hydroxycinnamic acid matrix and then spotted onto a MALDI plate. The spots were allowed to dry prior to analysis.

Enzymatic Assays. *Solid-Phase Digestion of Angiotensinogen-His_6-Beads in the Absence of Ni^{2+}-NTA Beads and Serum.* For the time-course experiments, 4 mg of dried resin was suspended in 50 mM MOPS buffer (1400 μL, pH 6.8) containing 0.18 mg mL^{-1} BSA. The suspension was equilibrated at 37 °C for 1.5 h with gentle shaking to ensure that the beads were swollen and dispersed. The reaction was started by the addition of renin solution (5U, 0.2U/μL). At regular intervals, 50 μL aliquots were withdrawn and immediately chilled on ice and then stored at 4 °C prior to HPLC, MS, or nanopore analysis. HPLC was used to determine the degree of proteolysis. The HPLC peak areas of released peptide were first normalized to the peak area of BSA and compared to a calibration curve. The quantity was corrected for the change in the concentration of peptide and protein due to the removal of aliquots in the assay.

Solid-Phase Digestion in the Presence of Human Serum and Ni^{2+}-NTA. An aliquot (200 μL) of the Ni^{2+}-NTA suspension (Qiagen) was centrifuged (10 min, 0.8 rpm) and resuspended in ddH_2O (1 mL). The beads were then washed twice with sodium phosphate buffer (100 mM, pH 7.4, 0.19 mg mL^{-1} BSA, 1 mL) using the same technique and then finally resuspended in 400 μL of buffer. The Ni^{2+}-NTA-bead suspension was combined with PEGA-angiotensinogenH_6 resin (4 mg) which had been washed. To the resultant suspension, human serum (125 μL) was added followed by renin solution (5U, 1.25U/μL). The mixture was incubated at 37 °C, with gentle shaking at 950 rpm for 18 h. The suspension was transferred to a QiaShredder spin column (the inner homogenizing frit removed) and centrifuged (30 s, 0.8 rpm) to separate the supernatant. The beads were washed with ddH_2O (7 × 500 μL) and wash solution (10 mM imidazole, 300 mM NaCl, 50 mM sodium phosphate, pH 7.99, 4 × 500 μL), followed by treatment with elution solution (250 mM imidazole, 200 mM NaCl, 50 mM sodium phosphate, pH 8.0, 4 × 500 μL). For these wash and elution steps, the beads were incubated for 1 min under gentle shaking, before centrifugation to collect each filtrate in a fresh tube. The eluted peptides were analyzed by sodium dodecyl sulfate-polyacrylamide gel electrophoresis (SDS-PAGE), HPLC and MALDI MS. For SDS-PAGE (12%), aliquots (10 μL) of each sample were mixed with an equal volume of loading buffer and run at 200 mV for 1 h. Gel bands were visualized by Coomassie Blue G-250 staining. The protein concentration of the serum was determined using the Bradford Protein Assay (Bio-Rad, Hercules, CA). Bovine serum albumin was used to generate a calibration curve. Each sample was analyzed in triplicate. Similarly, the peptide concentration was determined by integrating the peak areas in the HPLC chromatograms and comparison to a calibration curve setup with synthetic Ang-His_6 peptide. Two independent sample sets were analyzed.

Nanopore Recordings. Single-channel current recordings were performed by using a planar lipid bilayer apparatus as described.[50] Briefly, a bilayer of 1,2-diphytanoyl-*sn*-glycero-3-phosphocholine (Avanti Polar Lipids) was formed on an aperture (100 μm in diameter) in a Teflon septum (Goodfellow Corporation) separating the *cis* and *trans* chambers of the apparatus. Each compartment contained 1 M KCl, 50 mM Tris-HCl, pH 8.2, except for recordings with a salt gradient. Gel-purified heptameric αHL protein (final concentration 0.01−0.1 ng mL^{-1}) was added to the *cis* compartment to achieve insertion of a single channel into the bilayer. Subsequently, peptide-containing samples from the enzymatic digest or synthetic version were added to the *cis* side. Transmembrane currents were recorded at a holding potential of +100 mV (with the *cis* side grounded), unless stated otherwise, by using a patch−clamp amplifier (Axopatch 200B, Axon Instruments, Union City, CA). For analysis, currents were low-pass filtered at 10 kHz and sampled at 50 kHz using a Digidata 1200 A/D converter (Axon Instruments), as described.[12]

DOI: 10.1021/acs.analchem.5b01764
Anal. Chem. 2015, 87, 9149−9154

■ ASSOCIATED CONTENT

Supporting Information

Experimental procedures for the synthesis of soluble and resin-linked peptides, scientific data on the characterization of nanopore current blockades caused by (i) Ang-His_6 enzymatically released by renin from P-beads, (ii) synthetic Ang-His_6, and (iii) Ang-His_6 renin-cleaved from the P substrate beads and concomitant His-tag-purification, MALDI mass spectrum of Ang-His_6 after renin-digestion of P-beads and His-tag purification with N-beads, and a current trace of lipid bilayer membrane showing rupture due to human serum protein. The Supporting Information is available free of charge on the ACS Publications website at DOI: 10.1021/acs.analchem.5b01764.

■ AUTHOR INFORMATION

Corresponding Author

*E-mail: s.howorka@ucl.ac.uk.

Notes

The authors declare no competing financial interest.

■ ACKNOWLEDGMENTS

This work has been supported by the Engineering and Physical Science Research Council, The Royal Society of Chemistry, the Nuffield Foundation, and the Department of Chemistry at University College London. We thank Alethea Tabor for the use of a peptide synthesizer, Hagan Bayley and Ellina Mikhailova for providing α-hemolysin heptamer, and Kersti Karu for assistance in acquiring MS spectra.

■ REFERENCES

(1) Howorka, S.; Siwy, Z. *Chem. Soc. Rev.* **2009**, *38*, 2360−2384.
(2) Bayley, H.; Cremer, P. S. *Nature* **2001**, *413*, 226−230.
(3) Mayer, M.; Yang, J. *Acc. Chem. Res.* **2013**, *46*, 2998−3008.
(4) Wang, Y.; Zheng, D.; Tan, Q.; Wang, M. X.; Gu, L. Q. *Nat. Nanotechnol.* **2011**, *6*, 668−674.
(5) Shasha, C.; Henley, R. Y.; Stoloff, D. H.; Rynearson, K. D.; Hermann, T.; Wanunu, M. *ACS Nano* **2014**, *8*, 6425−6430.
(6) Jin, Q.; Fleming, A. M.; Ding, Y.; Burrows, C. J.; White, H. S. *Biochemistry* **2013**, *52*, 7870−7877.
(7) Yang, C.; Liu, L.; Zeng, T.; Yang, D.; Yao, Z.; Zhao, Y.; Wu, H. C. *Anal. Chem.* **2013**, *85*, 7302−7307.
(8) Wanunu, M.; Dadosh, T.; Ray, V.; Jin, J.; McReynolds, L.; Drndic, M. *Nat. Nanotechnol.* **2010**, *5*, 807−814.
(9) Cherf, G. M.; Lieberman, K. R.; Rashid, H.; Lam, C. E.; Karplus, K.; Akeson, M. *Nat. Biotechnol.* **2012**, *30*, 344−348.
(10) Manrao, E. A.; Derrington, I. M.; Laszlo, A. H.; Langford, K. W.; Hopper, M. K.; Gillgren, N.; Pavlenok, M.; Niederweis, M.; Gundlach, J. H. *Nat. Biotechnol.* **2012**, *30*, 349−353.
(11) Movileanu, L. *Trends Biotechnol.* **2009**, *27*, 333−341.
(12) Movileanu, L.; Howorka, S.; Braha, O.; Bayley, H. *Nat. Biotechnol.* **2000**, *18*, 1091−1095.
(13) Wei, R. S.; Gatterdam, V.; Wieneke, R.; Tampe, R.; Rant, U. *Nat. Nanotechnol.* **2012**, *7*, 257−263.
(14) Rotem, D.; Jayasinghe, L.; Salichou, M.; Bayley, H. *J. Am. Chem. Soc.* **2012**, *134*, 2781−2787.
(15) Zhao, Q.; de Zoysa, R. S.; Wang, D.; Jayawardhana, D. A.; Guan, X. *J. Am. Chem. Soc.* **2009**, *131*, 6324−6325.
(16) Zhao, Q.; Jayawardhana, D. A.; Wang, D.; Guan, X. *J. Phys. Chem. B* **2009**, *113*, 3572−3578.
(17) Kukwikila, M.; Howorka, S. *J. Phys.* **2010**, *22*, 454103.
(18) Movileanu, L.; Schmittschmitt, J. P.; Scholtz, J. M.; Bayley, H. *Biophys. J.* **2005**, *89*, 1030−1045.
(19) Wolfe, A. J.; Mohammad, M. M.; Cheley, S.; Bayley, H.; Movileanu, L. *J. Am. Chem. Soc.* **2007**, *129*, 14034−14041.
(20) Howorka, S.; Cheley, S.; Bayley, H. *Nat. Biotechnol.* **2001**, *19*, 636−639.
(21) Gu, L. Q.; Braha, O.; Conlan, S.; Cheley, S.; Bayley, H. *Nature* **1999**, *398*, 686−690.
(22) Halza, E.; Bro, T. H.; Bilenberg, B.; Kocer, A. *Anal. Chem.* **2013**, *85*, 811−815.
(23) Shim, J. W.; Gu, L. Q. *Anal. Chem.* **2007**, *79*, 2207−2213.
(24) Dekker, C. *Nat. Nanotechnol.* **2007**, *2*, 209−215.
(25) Miles, B. N.; Ivanov, A. P.; Wilson, K. A.; Dogan, F.; Japrung, D.; Edel, J. B. *Chem. Soc. Rev.* **2013**, *42*, 15−28.
(26) Geng, J.; Kim, K.; Zhang, J.; Escalada, A.; Tunuguntla, R.; Comolli, L. R.; Allen, F. I.; Shnyrova, A. V.; Cho, K. R.; Munoz, D.; Wang, Y. M.; Grigoropoulos, C. P.; Ajo-Franklin, C. M.; Frolov, V. A.; Noy, A. *Nature* **2014**, *514*, 612−615.
(27) Han, A.; Schurmann, G.; Mondin, G.; Bitterli, R. A.; Hegelbach, N. G.; de Rooij, N. F.; Staufer, R. *Appl. Phys. Lett.* **2006**, *88*, 093901.
(28) Fologea, D.; Ledden, B.; McNabb, D. S.; Li, J. *Appl. Phys. Lett.* **2007**, *91*, 053901.
(29) Hall, A. R.; Scott, A.; Rotem, D.; Mehta, K. K.; Bayley, H.; Dekker, C. *Nat. Nanotechnol.* **2010**, *5*, 874−877.
(30) Bell, N. A.; Engst, C. R.; Ablay, M.; Divitini, G.; Ducati, C.; Liedl, T.; Keyser, U. F. *Nano Lett.* **2012**, *12*, 512−517.
(31) Ondetti, M. A.; Cushman, D. W. *Annu. Rev. Biochem.* **1982**, *51*, 283−308.
(32) Hartman, D.; Sagnella, G. A.; Chesters, C. A.; Macgregor, G. A. *Clin. Chem.* **2004**, *50*, 2159−2161.
(33) Hollemans, H. J. G.; van der Meer, J.; Kloosterziel, W. *Clin. Chim. Acta* **1969**, *24*, 353−357.
(34) Corbett, A. D.; Gleason, J. L. *Tetrahedron Lett.* **2002**, *43*, 1369−1372.
(35) Poe, M.; Wu, J. K.; Lin, T. Y.; Hoogsteen, K.; Bull, H. G.; Slater, E. E. *Anal. Biochem.* **1984**, *140*, 459−467.
(36) Tewksbury, D. A.; Dart, R. A.; Travis, J. *Biochem. Biophys. Res. Commun.* **1981**, *99*, 1311−1315.
(37) Dhanaraj, V.; Dealwis, C. G.; Frazao, C.; Badasso, M.; Sibanda, B. L.; Tickle, I. J.; Cooper, J. B.; Driessen, H. P.; Newman, M.; Aguilar, C.; Wood, S. P.; Blundell, T. L.; Hobarth, P. M.; Geochegan, K. F.; Ammirati, M. J.; Danley, D. E.; O'Connor, B. A.; Hoover, D. J. *Nature* **1992**, *357*, 466−472.
(38) Wang, W.; Liang, T. C. *Biochemistry* **1994**, *33*, 14636−14641.
(39) Skegg, L. T.; Dorer, F. E.; Levine, M.; Lentz, K. E.; Kahn, J. R. *Adv. Exp. Med. Biol.* **1980**, *130*, 1−27.
(40) Deere, J.; De Oliveira, R. F.; Tomaszewski, B.; Millar, S.; Lalaouni, A.; Solares, L. F.; Flitsch, S. L.; Halling, P. J. *Langmuir* **2008**, *24*, 11762−11769.
(41) Basso, A.; De Martin, L.; Gardossi, L.; Margetts, G.; Brazendale, I.; Bosma, A. Y.; Ulijn, R. V.; Flitsch, S. L. *Chem. Commun.* **2003**, 1296−1297.
(42) Song, L.; Hobaugh, M. R.; Shustak, C.; Cheley, S.; Bayley, H.; Gouaux, J. E. *Science* **1996**, *274*, 1859−1866.
(43) Sutherland, T. C.; Long, Y. T.; Stefureac, R.; Bediako-Amoa, I.; Kraatz, H. B.; Lee, J. S. *Nano Lett.* **2004**, *4*, 1273−1277.
(44) Stefureac, R.; Long, Y. T.; Kraatz, H. B.; Howard, P.; Lee, J. S. *Biochemistry* **2006**, *45*, 9172−9179.
(45) Goodrich, C. P.; Kirmizialtin, S.; Huyghues-Despointes, B. M.; Zhu, A.; Scholtz, J. M.; Makarov, D. E.; Movileanu, L. *J. Phys. Chem. B* **2007**, *111*, 3332−3335.
(46) Meller, A.; Nivon, L.; Branton, D. *Phys. Rev. Lett.* **2001**, *86*, 3435−3438.
(47) Mathe, J.; Aksimentiev, A.; Nelson, D. R.; Schulten, K.; Meller, A. *Proc. Natl. Acad. Sci. U S A* **2005**, *102*, 12377−12382.
(48) Buchsbaum, S.; Mitchell, N.; Hugh, M.; Wiggin, M.; Marziali, A.; Coveney, P. V.; Ziwy, S.; Howorka, S. *Nano Lett.* **2013**, *13*, 3890−3896.
(49) Wanunu, M.; Morrison, W.; Rabin, Y.; Grosberg, A. Y.; Meller, A. *Nat. Nanotechnol.* **2010**, *5*, 160−165.
(50) Braha, O.; Walker, B.; Cheley, S.; Kasianowicz, J. J.; Song, L.; Gouaux, J. E.; Bayley, H. *Chem. Biol.* **1997**, *4*, 497−505.

DOI: 10.1021/acs.analchem.5b01764
Anal. Chem. 2015, 87, 9149−9154